Chem Catalysis

Article

Solvent-free photocatalytic propane oxidation to acetone with heterogenized decatungstate

Graphical abstract

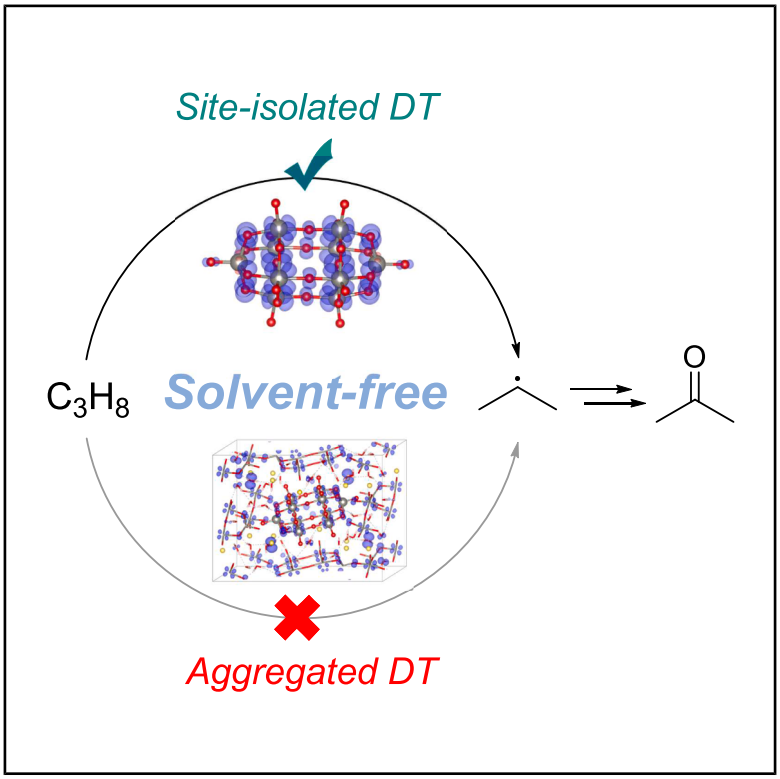

Highlights

- Isolated decatungstate (DT) enables solvent-free propane oxidation at ambient conditions
- Isolated DT retains molecular photocatalytic activity, whereas aggregated DT is inactive
- Spectroscopy and DFT studies reveal that site isolation is crucial to C–H activation

Authors

Yuhan Zhang, Jan Paul Menzel, Cristina Decavoli, ..., Victor S. Batista, Gary W. Brudvig, Dunwei Wang

Correspondence

dunwei.wang@bc.edu

In brief

The selective oxidation of light alkanes remains a long-standing challenge in catalysis. By immobilizing decatungstate as isolated active sites on SBA-15, Wang and colleagues enable solvent-free, room-temperature propane oxidation to acetone with high selectivity. Spectroscopy and DFT reveal that site isolation is crucial not only for maximizing accessibility but also for preserving the intrinsic photoreactivity, explaining the inactivity of aggregated DT. This work highlights the importance of molecular dispersion of active sites in heterogeneous catalysts and offers a sustainable route for propane valorization.

Zhang et al., 2026, Chem Catalysis 6, 101606
February 19, 2026 © 2025 Elsevier Inc. All rights are reserved, including those for text and data mining, AI training, and similar technologies.
https://doi.org/10.1016/j.checat.2025.101606

CellPress

Chem Catalysis

CellPress

Article

Solvent-free photocatalytic propane oxidation to acetone with heterogenized decatungstate

Yuhan Zhang,[1,5] Jan Paul Menzel,[2,5] Cristina Decavoli,[2] Xingxu Yan,[3] Rabiya Naveed,[1] Muchun Fei,[1] James R. Wilkes,[1] Min Li,[4] Yucheng Yuan,[1] Jier Huang,[1] Xiaoqing Pan,[3] Victor S. Batista,[2] Gary W. Brudvig,[2] and Dunwei Wang[1,6,*]

[1]Department of Chemistry, Boston College, 2609 Beacon Street, Chestnut Hill, MA 02467, USA
[2]Department of Chemistry, Yale University, 350 Edwards Street, New Haven, CT 06511, USA
[3]Department of Materials Science and Engineering, University of California, Irvine, 644F Engineering Tower, Irvine, CA 92697, USA
[4]West Campus Materials Characterization Core, Yale University, 810 West Campus Drive, New Haven, CT 06516, USA
[5]These authors contributed equally
[6]Lead contact
*Correspondence: dunwei.wang@bc.edu
https://doi.org/10.1016/j.checat.2025.101606

THE BIGGER PICTURE The selective oxidation of light alkanes into value-added liquid chemicals under mild conditions remains one of the long-standing challenges in catalysis. Light alkanes, such as methane, ethane, and propane, are naturally abundant yet chemically inert, and achieving their controlled functionalization would provide a transformative route to sustainable chemical manufacturing. Photocatalysis offers a promising strategy because photons can supply highly targeted energy inputs for bond activation. However, most heterogeneous photocatalysts generate dense electron-hole pairs upon excitation, which often leads to uncontrolled multielectron pathways and overoxidation. In contrast, molecular photocatalysts, such as decatungstate (DT), can perform precise hydrogen atom transfer, but their use has largely been restricted to homogeneous organic solvents, limiting scalability and green metrics.

This work demonstrates that immobilizing DT in a site-isolated manner on a mesoporous support can achieve both molecular-level precision and heterogeneous robustness. The resulting catalyst enables solvent-free oxidation of propane to acetone at room temperature and ambient pressure with high selectivity while avoiding the safety and separation concerns associated with organic solvents. Mechanistic and spectroscopic studies reveal that isolating active sites is crucial not only for exposing active sites but also for preserving the intrinsic photocatalytic reactivity of the molecular catalyst. Aggregated DT loses this reactivity, underscoring the importance of site isolation in selective photocatalytic C–H activation.

By bridging the conceptual gap between molecular precision and heterogeneous practicality, this work provides a generalizable strategy for designing photocatalysts capable of selective single-electron transformations, which is an essential requirement for upgrading light alkanes without overoxidation. These findings open up new opportunities for the sustainable valorization of abundant hydrocarbon resources and for expanding photocatalysis into large-scale chemical processes.

SUMMARY

The direct and selective oxidation of light alkanes into value-added liquid chemicals under mild conditions remains a long-standing challenge in catalysis. Here, we report a heterogeneous photocatalyst based on site-isolated decatungstate (DT) anions immobilized on SBA-15 via a silatrane linker (sil-DT). Under UV-light irradiation at room temperature and ambient pressure, the catalyst selectively oxidizes propane to acetone and exhibits an acetone production rate of 11.2 mmol g_{DT}^{-1} h^{-1}, a total liquid product selectivity of 89.0%, and an acetone fraction of 69.0% within the liquid products. In contrast, bulk sodium DT (NaDT) shows negligible activity under identical conditions. Spectroscopic and computational studies reveal that the high catalytic performance arises from the uniform dispersion and site isolation of DT species, which retain the photophysical properties of their homogeneous counterparts. This work demonstrates the critical role of molecular

All rights are reserved, including those for text and data mining, AI training, and similar technologies.

dispersion in enabling selective light-driven alkane oxidation and offers a sustainable route for propane valorization.

INTRODUCTION

Light alkanes, such as methane, ethane, and propane, are naturally abundant.[1–5] They generally feature high free energies, making it thermodynamically favorable to convert them into oxygenates as promising precursors for commodity chemical production.[6–10] Nevertheless, carrying out the direct conversion of alkanes to value-added oxygenates remains a challenge. Existing approaches often rely on processes that start from steam reforming, which is not only energy intensive but also prone to rapid catalyst deactivation.[11–15] At the heart of the issue is the difficulty in controlling the selectivity of C–H activation. The bond-dissociation energy (BDE) of the first C–H bond in a typical light alkane tends to be the highest. As a result, under thermochemical conditions, the energy needed for breaking the first C–H bond would also be sufficient to dissociate subsequent C–H bonds, leading to poor product selectivity.[9,16–18] Recognizing this issue, researchers have studied the possibility of substituting thermal energy with other forms of energy, including electricity or light.[3,19–21] Of these new approaches, photocatalysis is especially appealing because it directly uses photons to meet the energy requirements for activating bonds that are otherwise difficult to break. Although encouraging progress has been made in using photocatalysis for the synthesis of high-value chemicals, such as those of pharmaceutical significance, similar applications of photocatalysis to the synthesis of commodity chemicals have been lacking.[22–25]

Examinations of successful commercial implementations of photocatalytic conversion reveal that they typically feature molecular sensitizers or photocatalysts.[25–28] Thanks to the relatively slow recovery of these molecules after photoinduced charge transfer, the process is often limited to single-electron transfer. Consequently, substrate overactivation can be avoided. However, such molecular photocatalysts are mostly used for the synthesis of high-value molecules and would be cost prohibitive for the production of commodity chemicals. By comparison, heterogeneous photocatalysts are easy to prepare, recycle, and reuse and therefore hold great promise for scaled-up chemical synthesis.[29–33] However, they often feature energy bands and a relatively high density of charges upon photoexcitation. As a result, it has been exceedingly difficult to limit charge transfers from the photocatalyst to the reactive substrate to single electrons.[34] Hence, it remains a fundamental challenge to achieve high selectivity with heterogeneous photocatalysts for light alkane oxidation.

For the purpose of photocatalytic commodity chemical synthesis, one possible solution is to immobilize molecular catalysts onto heterogeneous supports.[35–38] As an isolated active site, the electronic energy levels are expected to be quantized, promising constrained charge transfers to minimize substrate overactivation. Polyoxometalates (POMs) are particularly suited for this role because they have been shown to serve as robust, well-defined molecular catalysts for reactions such as hydrogen atom transfer (HAT).[39–47] Among the studied POMs, decatungstate (DT; $[W_{10}O_{32}]^{4-}$) has demonstrated outstanding activity in the C–H bond activation of volatile alkanes via HAT.[48–50] Previous efforts to heterogenize DT mostly focused on improving its recyclability. Furthermore, these early demonstrations were generally still conducted in liquid-phase media with organic solvents, such as acetonitrile, which limits the prospect of scaling up for the sustainable synthesis of commodity chemicals.[51–55]

In this study, we built on this early research with the aim of achieving the site-isolated immobilization of DT. The target reaction was direct photocatalytic oxidation of propane to acetone under ambient, solvent-free gas-solid conditions with O_2 as the oxidant. Acetone is a widely used industrial solvent and precursor.[56,57] Its production from propane is not only a valuable transformation but also a representative model for studying C–H activation in the presence of O_2. We succeeded in achieving the highly selective synthesis of acetone. Notably, this synthesis was carried out without the use of any additional solvents. Moreover, when DT aggregates were used as a photocatalyst for the same synthesis, no appreciable propane activation was measured, further highlighting the importance of isolating the active centers.

RESULTS AND DISCUSSION

Synthesis and characterization of catalysts

We selected DT as the molecular photocatalyst because of its ease of synthesis, relatively good stability, and well-documented efficiency in promoting HAT under UV-light irradiation.[58–61] We prepared NaDT from $Na_2WO_4{\cdot}2H_2O$ and 1 M HCl ($10WO_4^{2-} + 16H^+ \rightarrow [W_{10}O_{32}]^{4-} + 8H_2O$) through a procedure modified from a previous report.[62] Once prepared, $[DT]^{4-}$ was immobilized onto mesoporous SBA-15 with a silatrane-based anchoring strategy (Figure 1A). In brief, we first synthesized 4-aminophenylsilatrane by reacting *p*-aminophenyltrimethoxysilane with triethanolamine, grafted it onto SBA-15, and then applied a mild acid treatment to remove the triethanolamine protecting group and protonate the amino linker.[63–65] We then immobilized $[DT]^{4-}$ via electrostatic interaction with surface-bound ammonium cations. The resulting sample, **sil-DT**, was expected to feature mostly isolated DT clusters. For comparison purposes, we prepared a second catalyst (**imp-NaDT**) via direct wet impregnation of sodium DT (NaDT) onto SBA-15.[51,53] This sample was expected to feature a mixture of isolated DT sites and some aggregates. We obtained a third catalyst (**mix-NaDT**) by physically mixing NaDT and SBA-15 through grinding. This sample was expected to feature mostly aggregates of NaDT on the surface of SBA-15 and a low degree of isolated sites. Lastly, we also synthesized bulk NaDT without adding any SBA-15.

Once synthesized, the catalysts were studied by scanning transmission electron microscopy (STEM) equipped with energy-dispersive X-ray spectroscopy (EDS) mapping (Figures 1B and S1). For **sil-DT**, W was well dispersed on the Si background (Figure S1), suggesting successful immobilization. Furthermore, the immobilization remained stable, as evidenced

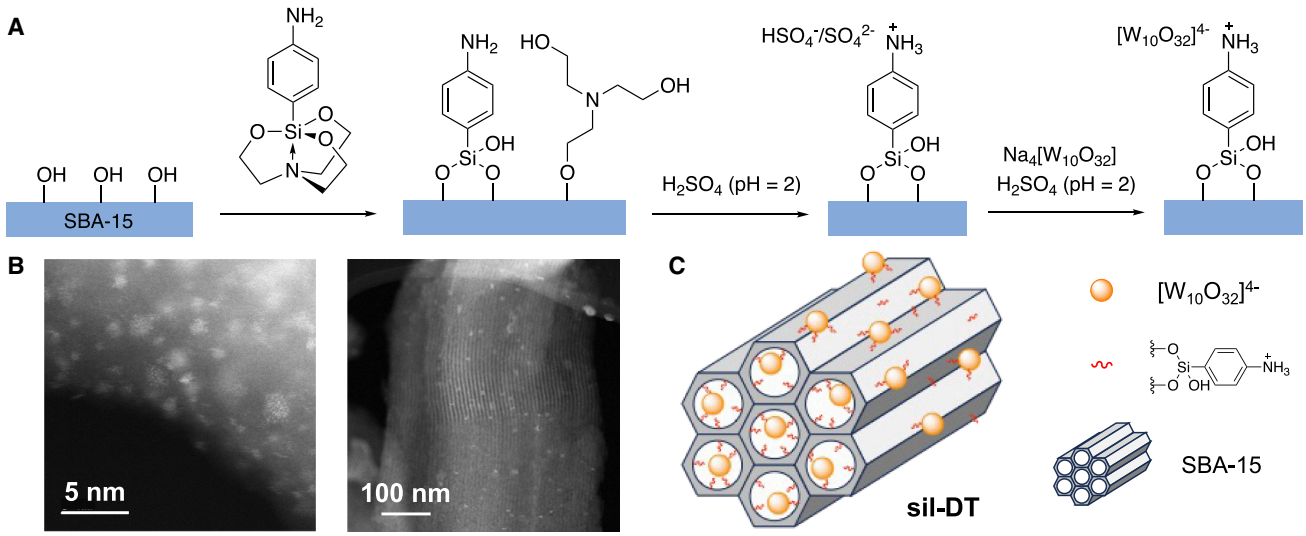

Figure 1. Preparation and characterization of sil-DT

(A) Procedure of **sil-DT** synthesis.

(B) STEM images of **sil-DT**.

(C) Schematic illustration of **sil-DT**.

by the absence of detachment or aggregation after rigorous rinsing. In contrast, the EDS mapping of **imp-NaDT** revealed partial aggregation of DT species, consistent with the absence of covalent anchoring and less controlled dispersion. For **mix-NaDT**, significant clustering and larger domains of W-rich regions were visible, supporting the expectation of substantial aggregation due to the physical mixing procedure. These structural characterizations confirmed that **sil-DT** predominantly features isolated DT, whereas **imp-NaDT** and **mix-NaDT** contain increasingly aggregated forms of DT. Inductively coupled plasma optical emission spectroscopy (ICP-OES) determined the loading density of DT to be 7.5 nmol mg^{-1} (1.8 wt %) in **sil-DT**, and on this basis, we prepared **imp-NaDT** and **mix-NaDT** with comparable DT loadings to ensure a meaningful comparison of their catalytic performance.

Photocatalytic performance for propane oxidation

Next, we carried out photocatalytic oxidation of propane at room temperature with a 365 nm light-emitting diode (LED; 485 mW/cm^2; Howsuper, H6015-S-6868-LG-365 nm) as the light source. For this set of experiments, a glass pressure reaction vessel (3 oz, Andrews Glass) with customized Swagelok reactor tops containing 80 mg of DT catalysts was filled with 1 bar air and 1 bar propane (Figure S2). In a typical experiment, we added D_2O to the reactor after 1 h of UV-light irradiation to extract the liquid product. With **sil-DT**, ^{1}H-NMR using DMSO as an internal standard detected 15.8 μmol of acetone. The yield corresponded to a normalized yield of 11.2 mmol g_{DT}^{-1} h^{-1}. Other detected products included isopropanol (4.6 mmol g_{DT}^{-1} h^{-1}), propanoic acid (0.4 mmol g_{DT}^{-1} h^{-1}), and acetic acid (0.03 mmol g_{DT}^{-1} h^{-1}). The total selectivity toward liquid oxygenates reached 81.0%, and acetone accounted for 69.0% of the total liquid products. No product was detected when the reaction was carried out without **sil-DT**, light, propane, or air. The results are summarized in Figures 2A and S3.

In stark contrast, no appreciable amount of liquid oxygenates was detected for bulk NaDT. Although oxygenates were detected on **imp-NaDT** (1.5 mmol g_{DT}^{-1} h^{-1} acetone, 2.4 mmol g_{DT}^{-1} h^{-1} isopropanol, 0.4 mmol g_{DT}^{-1} h^{-1} propanoic acid, and 0.4 mmol g_{DT}^{-1} h^{-1} acetic acid) and **mix-NaDT** (2.1 mmol g_{DT}^{-1} h^{-1} acetone, 1.1 mmol g_{DT}^{-1} h^{-1} isopropanol, 0.06 mmol g_{DT}^{-1} h^{-1} propanoic acid, and 0.06 mmol g_{DT}^{-1} h^{-1} acetic acid), their levels were significantly lower than those obtained on **sil-DT**.

A handful of catalytic systems for propane-to-acetone conversion have been reported previously. They either required high temperature or featured low conversion and/or selectivity.[66–70] For instance, using $FeCl_3$ as a photocatalyst, Teixeira and coworkers reported the photocatalytic oxidation of propane to acetone.[71] However, their system required CH_3CN as a solvent, limiting the prospect of scaling up. Within this context, our achievement of high selectivity for acetone formation in a solvent-free heterogeneous photocatalytic system is significant. Recognizing the outstanding performance of **sil-DT**, we focused the next set of experiments on this catalyst. Our first task was to demonstrate the recyclability of the catalyst by performing secondary and tertiary photocatalytic propane oxidation with recycled **sil-DT**. After the initial photocatalysis, we sequentially washed the spent catalyst with H_2SO_4 (pH 2) and acetonitrile, dried it under vacuum at 60°C, and then subjected the regenerated catalyst to the same reaction conditions. As shown in Figure 2B, we measured nearly identical activity for oxygenate formation. Repeating the recycling and photocatalysis procedure yielded comparable activity in the third cycle (Figure 2B). ICP-OES of the used **sil-DT** suggested negligible leaching of DT (7.3 $nmol_{DT}$ mg^{-1}), highlighting the robustness and reusability of the **sil-DT** catalyst.

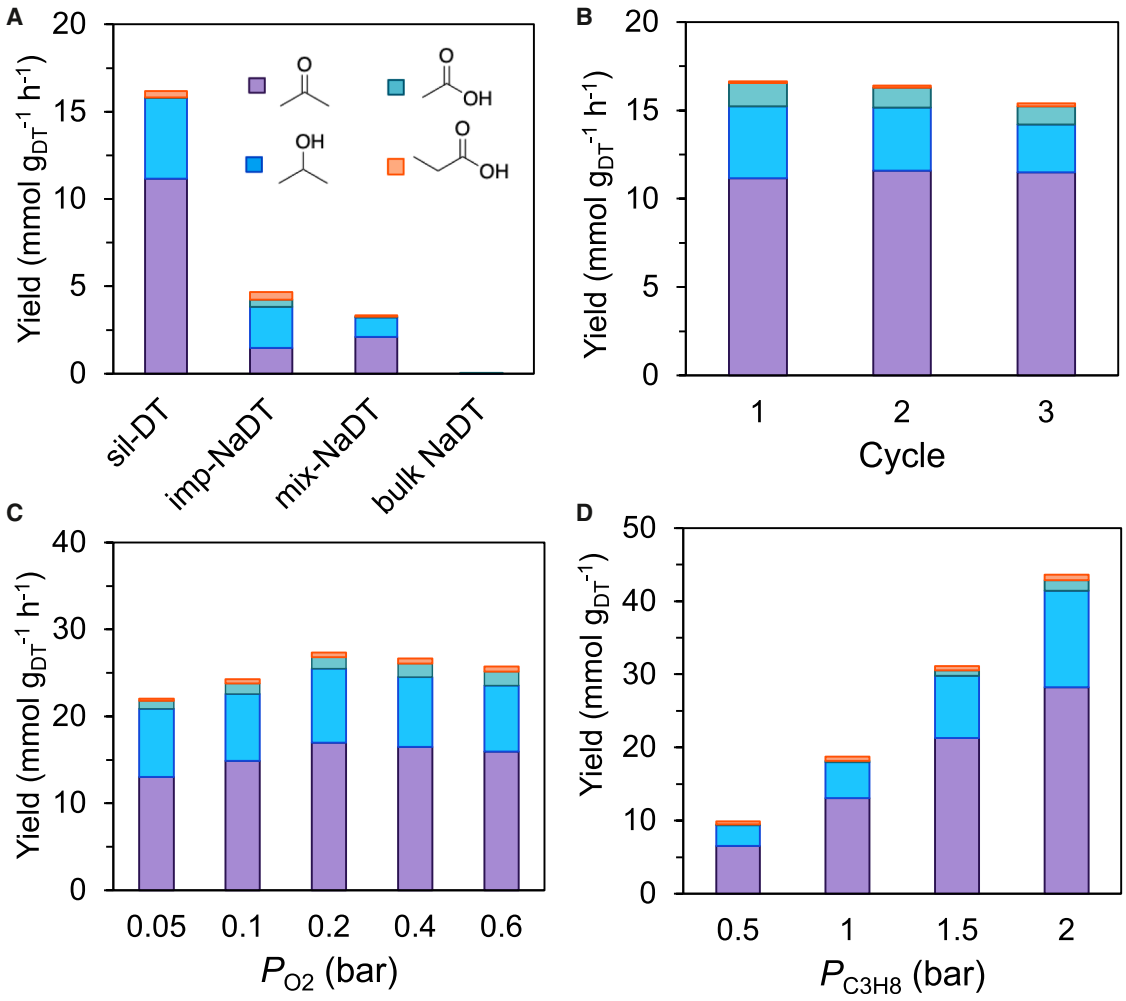

Figure 2. Catalytic performance of propane oxidation

(A) Comparison of different DT catalysts.

(B) Recyclability test.

(C) Test of the influence of O_2 partial pressures.

(D) Test of the influence of propane partial pressures.

All reactions in (B)–(D) were conducted in the presence of 10 mg **sil-DT** for 1 h. Refer to the main text for other experimental details.

We further investigated the effect of gaseous reactant partial pressures (Figures 2C and 2D). Increasing the O_2 partial pressure resulted in a modest improvement in propane conversion. However, when the O_2 partial pressure exceeded 0.2 bar, we observed a notable increase in CO_2 formation and a decline in liquid product yield, indicating enhanced overoxidation under oxygen-rich conditions (Figure S3). In contrast, increasing the partial pressure of propane led to a monotonic enhancement in product formation. These results suggest that C–H activation of propane, but not oxygen activation, is most likely rate limiting. This interpretation is consistent with our previous study on UV-light-driven propane dehydrogenation using $[DT]^{4-}$ in a homogeneous O_2-free system, which showed similar pressure-dependent behavior of propane.[72] Additionally, preliminary kinetic studies revealed that the reaction proceeded steadily over the first 3 h by maintaining a constant product formation rate and selectivity. For longer reaction durations, we observed a decline in liquid-product formation rates and increased CO_2 formation (Figure S3). This result could be attributed to overoxidation due to the accumulation of liquid products near active sites in the absence of solvent or significant vapor-phase removal. We envision that mitigation strategies such as continuous-flow reactor designs could be readily applied to address this issue and plan to carry them out in future studies. Together, these observations support the understanding that photoexcited DT is capable of activating propane directly under UV irradiation.

Investigation of the reaction mechanism

To further elucidate the reaction mechanism, we conducted density functional theory (DFT) calculations to investigate the complete reaction mechanism over **sil-DT** (Tables S1–S4). The photocatalytic cycle is initiated by the photoexcitation of DT,

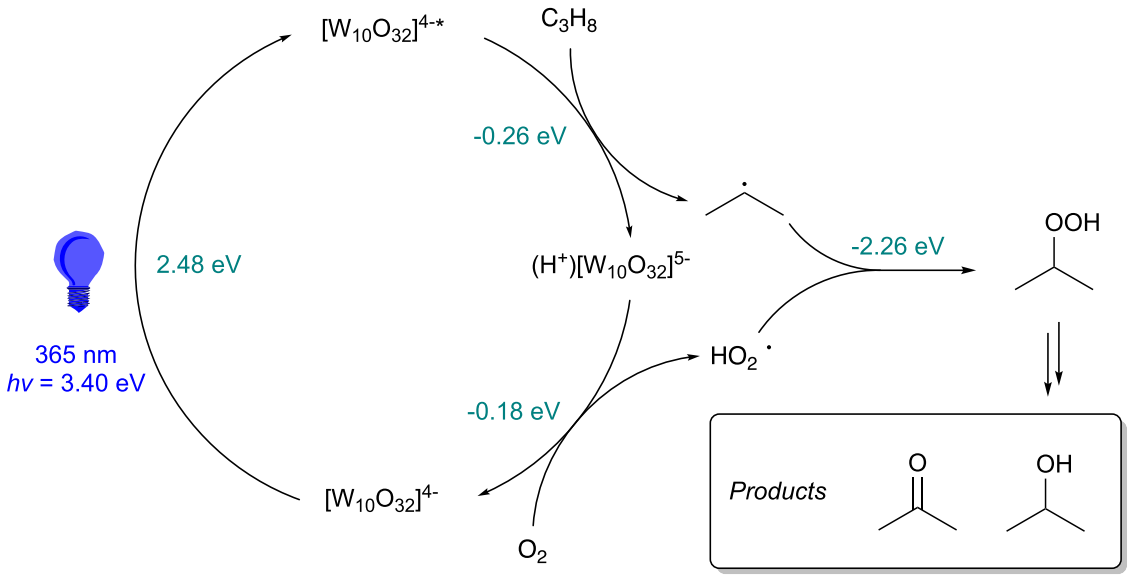

Figure 3. Catalytic cycle of propane oxidation over sil-DT

generating a reactive excited state ($[W_{10}O_{32}]^{4-*}$). This species undergoes HAT with propane to form a propyl radical and the reduced DT anion ($H^+[W_{10}O_{32}]^{5-}$). This HAT step is exergonic with calculated Gibbs free-energy changes of −0.26 eV. The reduced DT is then readily oxidized by molecular oxygen (ΔG = −0.18 eV), regenerating the original DT and producing a hydroperoxyl radical (·OOH). Subsequent radical recombination between the propyl radical and ·OOH to form propyl hydroperoxide is highly exergonic (ΔG = −2.26 eV) and is expected to dominate over alternative radical chain reactions as a result of steric confinement and restricted diffusion within the mesoporous SBA-15 channels. Finally, under UV-light irradiation, propyl hydroperoxide can be readily converted to isopropanol and acetone, a well-documented photochemical decomposition pathway for alkyl hydroperoxides.[68] It is worth noting that isopropanol can be further oxidized to acetone under the reaction conditions, as supported by control experiment using isopropanol as the sole substrate (Figures S6 and S7) and by previous reports on DT-catalyzed alcohol oxidation.[51,73] This proposed mechanism is schematically summarized in Figure 3.

Key role of site dispersion

The dispersion of active sites is widely acknowledged to affect catalytic efficiency by enhancing site accessibility.[74–79] However, the stark difference between **sil-DT** and bulk NaDT in their activity toward propane oxidation suggests that other critical insights are missing from this conventional view. Guided by this consideration, we next sought to investigate whether dispersion also modulates the intrinsic reactivity of a catalytic unit. UV-visible (UV-vis) diffuse reflectance spectroscopy (UV-vis DRS) revealed that **sil-DT** exhibited an absorption profile closely resembling that of dissolved NaDT (Figure 4A), suggesting that the DT units remain electronically isolated in the heterogenized state. It is therefore reasonable to expect them to behave like a dissolved molecule during photocatalysis. In contrast, bulk NaDT displayed a clear red shift in its absorption edge, indicative of significant electronic interactions between neighboring DT units in the solid state. Tauc plot analysis (Figure S4) further supported these observations. **sil-DT** and homogeneous DT ions exhibited a comparable optical band gap of 3.2 eV, whereas bulk NaDT featured a narrower band gap of 2.8 eV, consistent with the view that increased orbital overlap would result in a narrower band gap. X-ray photoelectron spectroscopy (XPS) further confirmed that DT aggregation in bulk NaDT leads to a higher valence-band maximum (VBM) and a lower conduction-band minimum (CBM) than the highest occupied molecular orbital (HOMO) and the lowest unoccupied molecular orbital (LUMO) of an isolated DT anion, respectively (Figure S8).

To further validate the difference in photochemical reactivity between **sil-DT** and bulk NaDT, we performed electron paramagnetic resonance (EPR) spectroscopy with cyclooctane as a model substrate and 5,5-dimethyl-1-pyrroline N-oxide (DMPO) as a spin agent (Figure S5). Upon 365 nm irradiation for 60 s, we observed a characteristic six-line EPR signal (g = 2.0059, $A_{N\beta}$ = 14.1 G, $A_{H\beta}$ = 22.2 G) in the presence of **sil-DT**; this can be assigned to the DMPO-cyclooctyl radical adduct. By comparison, no such signal was evident for the sample containing bulk NaDT under otherwise identical conditions. Control experiments confirmed that no signal was present in the absence of either light or **sil-DT**, indicating that the radical signal originated from a photoinduced HAT between **sil-DT** and cyclooctane. These findings further suggest that the dispersion of DT anions is key to the C–H activation in propane, whereas the aggregated form of DT is inactive under similar conditions (Figure 4B).

To understand the origin of the distinct catalytic behavior between **sil-DT** and bulk NaDT, we performed DFT calculations to evaluate their reactive states (Figure 5). Prior studies have established that the lowest triplet excited state (T_1) of DT formed after UV-light excitation and subsequent intersystem crossing is the active state responsible for HAT.[80–82] Our calculations showed

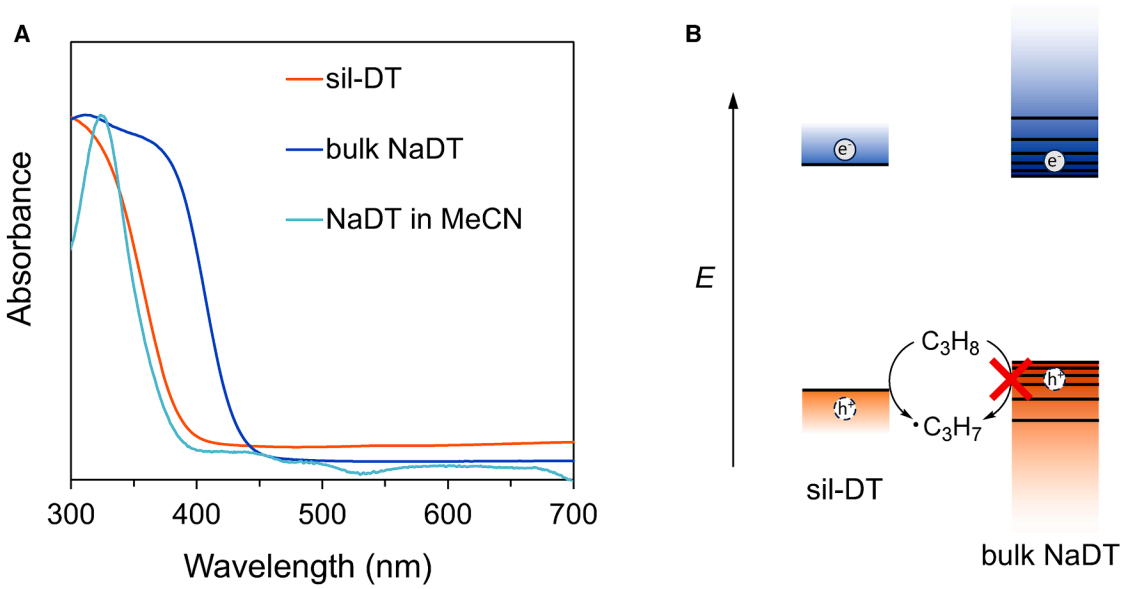

Figure 4. Investigation of band structures

(A) UV-vis DRS of **sil-DT** (red) and bulk NaDT (blue). Also presented is the UV-vis spectrum of NaDT dissolved in MeCN (light blue).

(B) Schematic diagram of band structures of **sil-DT** and bulk NaDT and their reactivity toward HAT with propane.

that in the isolated DT anion, the energy difference between the triplet and ground states was 2.39 eV; however, in the crystalline NaDT structure, the unpaired electrons in the triplet state were highly delocalized, resulting in a reduced triplet-state energy of 2.22 eV. This delocalization reduced the reactivity of the excited state toward HAT, consistent with the diminished catalytic performance observed for bulk NaDT and with our EPR spectroscopic studies, which showed that whereas **sil-DT** was capable of HAT from cyclooctane under UV-light irradiation, bulk NaDT was almost inactive. These findings further corroborate the differences observed in the UV-vis spectra of these two types of samples. Together, these results highlight the critical role of

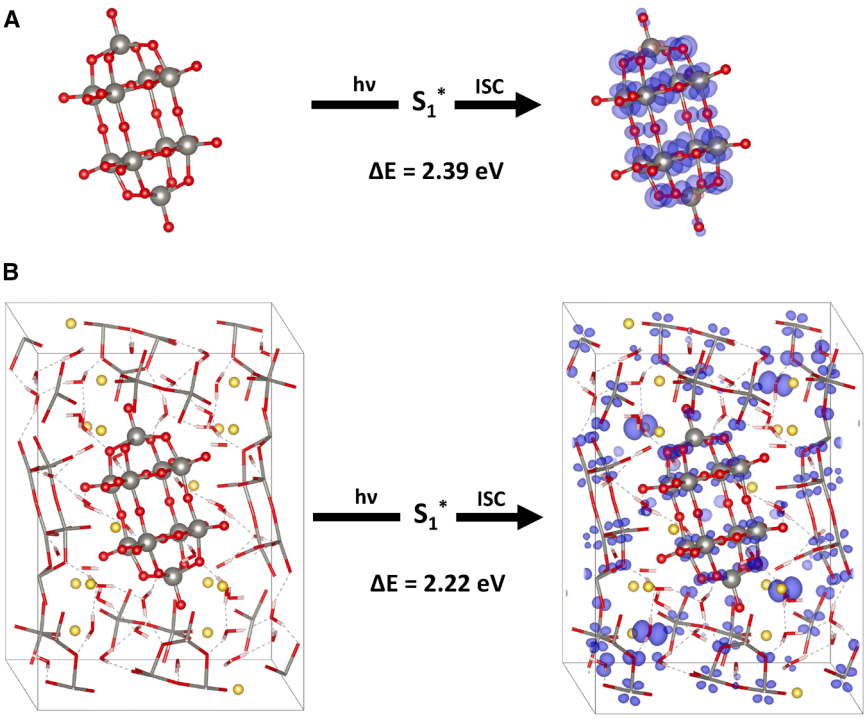

Figure 5. DFT calculations of the reactive states

(A) **Sil-DT**.

(B) NaDT.

active-site isolation in enhancing not only the accessibility but also the intrinsic reactivity of molecular photocatalysts.

Finally, we evaluated two in-between catalyst designs: **imp-DT** and **mix-DT**. Both samples exhibited modest catalytic activity that was significantly lower than that of **sil-DT** but higher than that of bulk NaDT (Figures 2A and S3). Although modestly higher dispersity of DT was expected from **imp-DT**, surface-area measurements (Table S5) revealed that this sample had a reduced surface area, presumably as a result of blocking by the impregnation treatment. Consequently, comparable photocatalytic performance was measured for **imp-DT** and **mix-DT**. Collectively, these data suggest that although some isolated DT sites are present and active in these samples, the coexistence of DT aggregates limits overall performance. These results further highlight the importance of precise control over DT dispersion and demonstrate that the silatrane-based strategy is an effective way to immobilize molecular catalysts and achieve a highly efficient, site-isolated heterogeneous catalyst.

Conclusion

In summary, we have developed a robust and efficient heterogeneous photocatalyst by anchoring site-isolated DT anions onto SBA-15 via silatrane linkers, enabling direct and selective oxidation of propane to acetone under mild conditions. The catalyst exhibits high activity and selectivity without the need for solvents, highlighting the potential for sustainable alkane functionalization. Mechanistic studies, supported by spectroscopy and DFT calculations, revealed that active-site isolation is crucial not only for maximizing accessibility but also for preserving the intrinsic photoreactivity. This work underscores the importance of the catalyst microenvironment in controlling product selectivity and provides a blueprint for designing molecularly defined photocatalysts for light alkane valorization. Future development of continuous-flow systems and visible-light-responsive analogs are likely to further expand the practical applicability of this strategy in green chemical manufacturing.

METHODS

Detailed methods are provided in the supplemental information.

RESOURCE AVAILABILITY

Lead contact

Requests for further information and resources should be directed to and will be fulfilled by the lead contact, Dunwei Wang (dunwei.wang@bc.edu).

Materials availability

All reagents and materials in this study are either commercially available or can be synthesized according to the procedures reported in the supplemental information.

Data and code availability

All data reported in this paper are available in the article and the supplemental information or will be shared by the lead contact upon request.

ACKNOWLEDGMENTS

This work was primarily supported by the National Science Foundation (NSF) under awards CHE-1955098 and CHE-2154928. NMR-related studies were supported by the NSF MRI program (CHE-2117246) and the National Institutes of Health (NIH) HEI-S10 award (1S10OD026910-01A1). The authors gratefully acknowledge Prof. Matthias Waegele, Dr. Jing Jin, and Dr. Thacien Ngendahimana at Boston College for their assistance with gas chromatography, UV-vis spectroscopy, and EPR measurements, respectively. They also thank the Yale West Campus Materials Characterization Core for instrumental support. They acknowledge the use of facilities and instrumentation at the UC Irvine Materials Research Institute (IMRI), supported in part by the NSF through the UC Irvine MRSEC program (DMR-2011967).

AUTHOR CONTRIBUTIONS

Y.Z. and J.P.M. contributed equally to this work. Y.Z. designed and performed the experiments and analyzed the data. Y.Z. and D.W. wrote the initial draft of the manuscript and performed subsequent revisions. J.P.M. carried out the DFT calculations. C.D. and M.F. synthesized the silatrane precursor. X.Y. performed the STEM and EDS measurements. R.N. assisted with the experiments. J.R.W. and M.L. conducted the XPS studies, and M.L. analyzed the data. Y.Y. provided constructive guidance and helped coordinate collaborations. J.H. provided UV-vis instrumentation and guidance. X.P., V.S.B., G.W.B., and D.W. supervised the project, secured funding, and contributed to discussions and manuscript refinement.

DECLARATION OF INTERESTS

The authors declare no competing interests.

SUPPLEMENTAL INFORMATION

Supplemental information can be found online at https://doi.org/10.1016/j.checat.2025.101606.

Received: October 4, 2025
Revised: November 10, 2025
Accepted: December 4, 2025
Published: February 12, 2026

REFERENCES

1. Li, X., Pei, C., and Gong, J. (2021). Shale gas revolution: Catalytic conversion of C1–C3 light alkanes to value-added chemicals. Chem *7*, 1755–1801. https://doi.org/10.1016/j.chempr.2021.02.002.
2. Pulcinella, A., Mazzarella, D., and Noël, T. (2021). Homogeneous catalytic C(sp^3)–H functionalization of gaseous alkanes. Chem. Commun. *57*, 9956–9967. https://doi.org/10.1039/D1CC04073A.
3. Li, X., Wang, C., and Tang, J. (2022). Methane transformation by photocatalysis. Nat. Rev. Mater. *7*, 617–632. https://doi.org/10.1038/s41578-022-00422-3.
4. Forde, M.M., Armstrong, R.D., Hammond, C., He, Q., Jenkins, R.L., Kondrat, S.A., Dimitratos, N., Lopez-Sanchez, J.A., Taylor, S.H., Willock, D., et al. (2013). Partial oxidation of ethane to oxygenates using Fe- and Cu-containing ZSM-5. J. Am. Chem. Soc. *135*, 11087–11099. https://doi.org/10.1021/ja403060n.
5. Li, F., Wang, B., Chen, X., Lai, Y., Wang, T., Fan, H., Yang, X., and Guo, Q. (2022). Photocatalytic oxidative dehydrogenation of propane for selective propene production with TiO_2. JACS Au *2*, 2607–2616. https://doi.org/10.1021/jacsau.2c00512.
6. Grant, J.T., Venegas, J.M., McDermott, W.P., and Hermans, I. (2018). Aerobic oxidations of light alkanes over solid metal oxide catalysts. Chem. Rev. *118*, 2769–2815. https://doi.org/10.1021/acs.chemrev.7b00236.
7. Hall, J.N., Li, M., and Bollini, P. (2022). Light alkane oxidation over well-defined active sites in metal–organic framework materials. Catal. Sci. Technol. *12*, 418–435. https://doi.org/10.1039/D1CY01876K.
8. Martin, R., Kim, M., Asthagiri, A., and Weaver, J.F. (2021). Alkane activation and oxidation on late-transition-metal oxides: Challenges and

opportunities. ACS Catal. *11*, 4682–4703. https://doi.org/10.1021/acscatal.1c00612.

9. Sun, M., Zhang, J., Putaj, P., Caps, V., Lefebvre, F., Pelletier, J., and Basset, J.-M. (2014). Catalytic oxidation of light alkanes (C1–C4) by heteropoly compounds. Chem. Rev. *114*, 981–1019. https://doi.org/10.1021/cr300302b.
10. Chan, S.I., Yu, S.S.-F., Liu, C.-C., and Mou, C.-Y. (2020). Selective oxidation of light alkanes under mild conditions. Curr. Opin. Green Sustainable Chem. *22*, 39–46. https://doi.org/10.1016/j.cogsc.2019.12.003.
11. Ighalo, J.O., and Amama, P.B. (2024). Recent advances in the catalysis of steam reforming of methane (SRM). Int. J. Hydrogen Energy *51*, 688–700. https://doi.org/10.1016/j.ijhydene.2023.10.177.
12. Iulianelli, A., Liguori, S., Wilcox, J., and Basile, A. (2016). Advances on methane steam reforming to produce hydrogen through membrane reactors technology: A review. Catal. Rev. *58*, 1–35. https://doi.org/10.1080/01614940.2015.1099882.
13. Angeli, S.D., Monteleone, G., Giaconia, A., and Lemonidou, A.A. (2014). State-of-the-art catalysts for CH_4 steam reforming at low temperature. Int. J. Hydrogen Energy *39*, 1979–1997. https://doi.org/10.1016/j.ijhydene.2013.12.001.
14. Zhang, H., Sun, Z., and Hu, Y.H. (2021). Steam reforming of methane: Current states of catalyst design and process upgrading. Renew. Sustain. Energy Rev. *149*, 111330. https://doi.org/10.1016/j.rser.2021.111330.
15. Sanna, A., Openshaw, D., Oghotomo, P., and Bagnato, G. (2025). Steam reforming of methane: State of the art and novel technologies. React. Chem. Eng. *10*, 1963–1977. https://doi.org/10.1039/D5RE00001G.
16. Xu, Z.C., and Park, E.D. (2022). Gas-phase selective oxidation of methane into methane oxygenates. Catalysts *12*, 314. https://doi.org/10.3390/catal12030314.
17. Meng, X., Cui, X., Rajan, N.P., Yu, L., Deng, D., and Bao, X. (2019). Direct methane conversion under mild condition by thermo-electro-or photocatalysis. Chem *5*, 2296–2325. https://doi.org/10.1016/j.chempr.2019.05.008.
18. Wang, Y., Hu, P., Yang, J., Zhu, Y.-A., and Chen, D. (2021). C–H bond activation in light alkanes: A theoretical perspective. Chem. Soc. Rev. *50*, 4299–4358. https://doi.org/10.1039/D0CS01262A.
19. Jiang, Y., Li, S., Fan, Y., and Tang, Z. (2024). Best practices for experiments and reports in photocatalytic methane conversion. Angew. Chem. *63*, e202404658. https://doi.org/10.1002/ange.202404658.
20. Song, H., Meng, X., Wang, S., Zhou, W., Wang, X., Kako, T., and Ye, J. (2019). Direct and selective photocatalytic oxidation of CH_4 to oxygenates with O_2 on cocatalysts/ZnO at room temperature in water. J. Am. Chem. Soc. *141*, 20507–20515. https://doi.org/10.1021/jacs.9b11440.
21. Zhou, M., and Wang, H. (2022). Optimally selecting photo- and electrocatalysis to facilitate CH_4 activation on TiO_2(110) surface: Localized photoexcitation versus global electric-field polarization. JACS Au *2*, 188–196. https://doi.org/10.1021/jacsau.1c00466.
22. Corrigan, N., Shanmugam, S., Xu, J., and Boyer, C. (2016). Photocatalysis in organic and polymer synthesis. Chem. Soc. Rev. *45*, 6165–6212. https://doi.org/10.1039/C6CS00185H.
23. Akita, M., Ceroni, P., Stephenson, C.R.J., and Masson, G. (2023). Progress in photocatalysis for organic chemistry. J. Org. Chem. *88*, 6281–6283. https://doi.org/10.1021/acs.joc.3c00812.
24. Marzo, L., Pagire, S.K., Reiser, O., and König, B. (2018). Visible-light photocatalysis: Does it make a difference in organic synthesis? Angew. Chem. Int. Ed. *57*, 10034–10072. https://doi.org/10.1002/anie.201709766.
25. Michelin, C., and Hoffmann, N. (2018). Photosensitization and photocatalysis—Perspectives in organic synthesis. ACS Catal. *8*, 12046–12055. https://doi.org/10.1021/acscatal.8b03050.
26. De Bonfils, P., Péault, L., Nun, P., and Coeffard, V. (2021). State of the art of bodipy-based photocatalysts in organic synthesis. Eur. J. Org. Chem. *2021*, 1809–1824. https://doi.org/10.1002/ejoc.202001446.
27. Leung, C.-F., and Lau, T.-C. (2021). Organic photosensitizers for catalytic solar fuel generation. Energy Fuels *35*, 18888–18899. https://doi.org/10.1021/acs.energyfuels.1c02675.
28. Cheng, S., Tang, J., and Quan, Y. (2022). Metal-organic frameworks with organic photosensitizers in organic synthesis. Eur. J. Inorg. Chem. *2022*, e202200274. https://doi.org/10.1002/ejic.202200274.
29. Fox, M.A., and Dulay, M.T. (1993). Heterogeneous photocatalysis. Chem. Rev. *93*, 341–357. https://doi.org/10.1021/cr00017a016.
30. Gisbertz, S., and Pieber, B. (2020). Heterogeneous photocatalysis in organic synthesis. ChemPhotoChem *4*, 456–475. https://doi.org/10.1002/cptc.202000014.
31. Parrino, F., and Palmisano, G. (2020). Highlights on recent developments of heterogeneous and homogeneous photocatalysis. Molecules *26*, 23. https://doi.org/10.3390/molecules26010023.
32. Ibhadon, A., and Fitzpatrick, P. (2013). Heterogeneous photocatalysis: Recent advances and applications. Catalysts *3*, 189–218. https://doi.org/10.3390/catal3010189.
33. Friend, C.M., and Xu, B. (2017). Heterogeneous catalysis: A central science for a sustainable future. Acc. Chem. Res. *50*, 517–521. https://doi.org/10.1021/acs.accounts.6b00510.
34. Kou, J., Lu, C., Wang, J., Chen, Y., Xu, Z., and Varma, R.S. (2017). Selectivity enhancement in heterogeneous photocatalytic transformations. Chem. Rev. *117*, 1445–1514. https://doi.org/10.1021/acs.chemrev.6b00396.
35. Choplin, A., and Quignard, F. (1998). From supported homogeneous catalysts to heterogeneous molecular catalysts. Coord. Chem. Rev. *178–180*, 1679–1702. https://doi.org/10.1016/S0010-8545(98)00062-9.
36. Mak, C.H., Han, X., Du, M., Kai, J.-J., Tsang, K.F., Jia, G., Cheng, K.-C., Shen, H.-H., and Hsu, H.-Y. (2021). Heterogenization of homogeneous photocatalysts utilizing synthetic and natural support materials. J. Mater. Chem. A *9*, 4454–4504. https://doi.org/10.1039/D0TA08334H.
37. Qi, Y., Sun, H., She, P., Qin, J.-S., and Rao, H. (2024). Molecular heterogeneous photocatalysts for visible-light-driven CO_2 reduction. Chem. Rec. *25*, e202400202. https://doi.org/10.1002/tcr.202400202.
38. Liu, X., Inagaki, S., and Gong, J. (2016). Heterogeneous molecular systems for photocatalytic CO_2 reduction with water oxidation. Angew. Chem. Int. Ed. *55*, 14924–14950. https://doi.org/10.1002/anie.201600395.
39. Cherevan, A.S., Nandan, S.P., Roger, I., Liu, R., Streb, C., and Eder, D. (2020). Polyoxometalates on functional substrates: Concepts, synergies, and future perspectives. Adv. Sci. *7*, 1903511. https://doi.org/10.1002/advs.201903511.
40. Ye, J.-J., and Wu, C.-D. (2016). Immobilization of polyoxometalates in crystalline solids for highly efficient heterogeneous catalysis. Dalton Trans. *45*, 10101–10112. https://doi.org/10.1039/C6DT01378C.
41. Ji, Y., Huang, L., Hu, J., Streb, C., and Song, Y.-F. (2015). Polyoxometalate-functionalized nanocarbon materials for energy conversion, energy storage and sensor systems. Energy Environ. Sci. *8*, 776–789. https://doi.org/10.1039/C4EE03749A.
42. Zhou, Y., Chen, G., Long, Z., and Wang, J. (2014). Recent advances in polyoxometalate-based heterogeneous catalytic materials for liquid-phase organic transformations. RSC Adv. *4*, 42092–42113. https://doi.org/10.1039/C4RA05175K.
43. Kozhevnikov, I.V. (1998). Catalysis by heteropoly acids and multicomponent polyoxometalates in liquid-phase reactions. Chem. Rev. *98*, 171–198. https://doi.org/10.1021/cr960400y.
44. Zhang, Z., Cheng, F., Ma, X., Sun, K., Huang, X., An, J., Peng, M., Chen, X., and Yu, B. (2024). Decatungstate-photocatalyzed direct acylation of N-heterocycles with aldehydes. Green Chem. *26*, 7331–7336. https://doi.org/10.1039/D4GC00534A.
45. Qiao, L., Yang, W., Zhao, X., Li, E., Chen, X., Qu, L., and Yu, B. (2024). Decatungstate-photocatalyzed radical addition of C(sp^3)–H to azauracils. Org. Chem. Front. *11*, 5791–5797. https://doi.org/10.1039/D4QO01339E.

46. Babawale, F., Ghosh, I., and König, B. (2025). photo-catalyzed synthesis of indanones from aromatic aldehydes and terminal alkynes. J. Org. Chem. *90*, 13885–13890. https://doi.org/10.1021/acs.joc.5c01749.

47. Wu, X., Zhou, J., Hu, Z., and Xu, T. (2024). Photoinduced radical addition process enables deoxygenative hydroacylation and hydrophosphonylation of carbonyls. Chem Catal. *4*, 100828. https://doi.org/10.1016/j.checat.2023.100828.

48. Laudadio, G., Govaerts, S., Wang, Y., Ravelli, D., Koolman, H.F., Fagnoni, M., Djuric, S.W., and Noël, T. (2018). Selective C(sp^3)–H aerobic oxidation enabled by decatungstate photocatalysis in flow. Angew. Chem. Int. Ed. *57*, 4078–4082. https://doi.org/10.1002/anie.201800818.

49. Laudadio, G., Deng, Y., van der Wal, K., Nuño, M., Fagnoni, M., Guthrie, D., Sun, Y., and Noël, T. (2020). C(sp^3)–H functionalizations of light hydrocarbons using decatungstate photocatalysis in flow. Science *369*, 92–96. https://doi.org/10.1126/science.abb4688.

50. Musgrave, C.B., III, Olsen, K., Liebov, N.S., Groves, J.T., Goddard, W.A., III, and Gunnoe, T.B. (2023). Partial oxidation of methane enabled by decatungstate photocatalysis coupled to free radical chemistry. ACS Catal. *13*, 6382–6395. https://doi.org/10.1021/acscatal.3c00750.

51. Maldotti, A., Molinari, A., Varani, G., Lenarda, M., Storaro, L., Bigi, F., Maggi, R., Mazzacani, A., and Sartori, G. (2002). Immobilization of (n-$Bu_4N)_4W_{10}O_{32}$ on mesoporous MCM-41 and amorphous silicas for photocatalytic oxidation of cycloalkanes with molecular oxygen. J. Catal. *209*, 210–216. https://doi.org/10.1006/jcat.2002.3618.

52. Molinari, A., Maldotti, A., Bratovcic, A., and Magnacca, G. (2013). Photocatalytic properties of sodium decatungstate supported on sol–gel silica in the oxidation of glycerol. Catal. Today *206*, 46–52. https://doi.org/10.1016/j.cattod.2011.11.033.

53. Molinari, A., Amadelli, R., Carassiti, V., and Maldotti, A. (2000). Photocatalyzed oxidation of cyclohexene and cyclooctene with (n-$Bu_4N)_4W_{10}O_{32}$ and (n-$Bu_4N)_4W_{10}O_{32}$/Fe^{III}[*meso*-tetrakis(2,6-dichlorophenyl)porphyrin] in homogeneous and heterogeneous systems. Eur. J. Inorg. Chem. *2000*, 91–96. https://doi.org/10.1002/(SICI)1099-0682(200001)2000:1%3C91::AID-EJIC91%3E3.0.CO;2-J.

54. Molinari, A., Amadelli, R., Mazzacani, A., Sartori, G., and Maldotti, A. (2002). Tetralkylammonium and Sodium Decatungstate Heterogenized on silica: Effects of the nature of cations on the photocatalytic oxidation of organic substrates. Langmuir *18*, 5400–5405. https://doi.org/10.1021/la0110141.

55. Tzirakis, M.D., Lykakis, I.N., and Orfanopoulos, M. (2009). Decatungstate as an efficient photocatalyst in organic chemistry. Chem. Soc. Rev. *38*, 2609–2621. https://doi.org/10.1039/B812100C.

56. Bui, L., Chakrabarti, R., and Bhan, A. (2016). Mechanistic origins of unselective oxidation products in the conversion of propylene to acrolein on $Bi_2Mo_3O_{12}$. ACS Catal. *6*, 6567–6580. https://doi.org/10.1021/acscatal.6b01830.

57. Zakoshansky, V.M. (2007). The cumene process for phenol-acetone production. Petrol. Chem. *47*, 273–284. https://doi.org/10.1134/S096554410704007X.

58. Tanielian, C. (1998). Decatungstate photocatalysis. Coord. Chem. Rev. *178–180*, 1165–1181. https://doi.org/10.1016/S0010-8545(98)00160-X.

59. Hong, B.-C., and Indurmuddam, R.R. (2024). Tetrabutylammonium decatungstate (TBADT), a compelling and trailblazing catalyst for visible-light-induced organic photocatalysis. Org. Biomol. Chem. *22*, 3799–3842. https://doi.org/10.1039/D4OB00171K.

60. Singh, P.P., Sinha, S., Gahtori, P., Tivari, S., and Srivastava, V. (2024). Recent advances of decatungstate photocatalyst in HAT process. Org. Biomol. Chem. *22*, 2523–2538. https://doi.org/10.1039/D4OB00213J.

61. Ravelli, D., Protti, S., and Fagnoni, M. (2016). Decatungstate anion for photocatalyzed "window ledge" reactions. Acc. Chem. Res. *49*, 2232–2242. https://doi.org/10.1021/acs.accounts.6b00339.

62. Duncan, D.C., Netzel, T.L., and Hill, C.L. (1995). Early-time dynamics and reactivity of polyoxometalate excited states. Identification of a short-lived LMCT excited state and a reactive long-lived charge-transfer intermediate following picosecond flash excitation of $[W_{10}O_{32}]^{4-}$ in acetonitrile. Inorg. Chem. *34*, 4640–4646. https://doi.org/10.1021/ic00122a021.

63. Troiano, J.L., Crabtree, R.H., and Brudvig, G.W. (2022). Optimization of surface loading of the silatrane anchoring group on TiO_2. ACS Appl. Mater. Interfaces *14*, 6582–6589. https://doi.org/10.1021/acsami.1c20678.

64. Troiano, J.L., Hu, G., Crabtree, R.H., and Brudvig, G.W. (2020). Diazo coupling for surface attachment of small molecules to TiO2 nanoparticles. Chem. Commun. *56*, 9340–9343. https://doi.org/10.1039/D0CC03631E.

65. Brennan, B.J., Gust, D., and Brudvig, G.W. (2014). Organosilatrane building blocks. Tetrahedron Lett. *55*, 1062–1064. https://doi.org/10.1016/j.tetlet.2013.12.082.

66. Bravo-Suárez, J.J., Bando, K.K., Akita, T., Fujitani, T., Fuhrer, T.J., and Oyama, S.T. (2008). Propane reacts with O_2 and H_2 on gold supported TS-1 to form oxygenates with high selectivity. Chem. Commun. *3272*. https://doi.org/10.1039/b800620b.

67. Ma, X., Yin, H., Pu, Z., Zhang, X., Hu, S., Zhou, T., Gao, W., Luo, L., Li, H., and Zeng, J. (2024). Propane wet reforming over PtSn nanoparticles on γ-Al_2O_3 for acetone synthesis. Nat. Commun. *15*, 8470. https://doi.org/10.1038/s41467-024-52702-x.

68. Xu, J., Mojet, B., Vanommen, J., and Lefferts, L. (2005). Effects of Brønsted acidity in the mechanism of selective oxidation of propane to acetone on CaY zeolite at room temperature. J. Catal. *232*, 411–423. https://doi.org/10.1016/j.jcat.2005.04.004.

69. Marcinkowska, K., Kaliaguine, S., and Roberge, P.C. (1984). Photocatalytic oxidation of propane by oxygen on supported $MoSiO_2$ catalysts. J. Catal. *90*, 49–58. https://doi.org/10.1016/0021-9517(84)90083-6.

70. Yang, C.-H., Liu, X.-C., Li, Y., Yuan, S., Wang, T., Zhou, Z.-Y., and Sun, S.-G. (2023). Selective conversion of propane by electrothermal catalysis in proton exchange membrane fuel cell. ChemSusChem *16*, e202300699. https://doi.org/10.1002/cssc.202300699.

71. Rogolino, A., Filho, J.B.G., Fritsch, L., Ardisson, J.D., da Silva, M.A.R., Atta Diab, G.A., Silva, I.F., Moraes, C.A.F., Forim, M.R., Bauer, M., et al. (2023). Direct synthesis of acetone by aerobic propane oxidation promoted by photoactive iron(III) chloride under mild conditions. ACS Catal. *13*, 8662–8669. https://doi.org/10.1021/acscatal.3c02092.

72. Yuan, Y., Zhang, Y., Menzel, J.P., Santoro, J., Dolack, M., Wang, H., Batista, V., and Wang, D. (2024). High-conversion propane dehydrogenation by photocatalysis under ambient conditions. ACS Catal. *14*, 17445–17452. https://doi.org/10.1021/acscatal.4c06192.

73. Bonchio, M., Carraro, M., Scorrano, G., Fontananova, E., and Drioli, E. (2003). Heterogeneous photooxidation of alcohols in water by photocatalytic membranes incorporating decatungstate. Adv. Synth. Catal. *345*, 1119–1126. https://doi.org/10.1002/adsc.200303076.

74. Khandelwal, A., Maarisetty, D., and Baral, S.S. (2022). Fundamentals and application of single-atom photocatalyst in sustainable energy and environmental applications. Renew. Sustain. Energy Rev. *167*, 112693. https://doi.org/10.1016/j.rser.2022.112693.

75. Gao, C., Low, J., Long, R., Kong, T., Zhu, J., and Xiong, Y. (2020). Heterogeneous single-atom photocatalysts: Fundamentals and applications. Chem. Rev. *120*, 12175–12216. https://doi.org/10.1021/acs.chemrev.9b00840.

76. Wei, T., Zhou, J., and An, X. (2024). Recent advances in single-atom catalysts (SACs) for photocatalytic applications. Mater. Rep. Energy *4*, 100285. https://doi.org/10.1016/j.matre.2024.100285.

77. Li, C.F., Pan, W.G., Zhang, Z.R., Wu, T., and Guo, R.T. (2023). Recent progress of single-atom photocatalysts applied in energy conversion and environmental protection. Small *19*, 2300460. https://doi.org/10.1002/smll.202300460.

78. Wu, S.-M., and Schmuki, P. (2025). Single atom cocatalysts in photocatalysis. Adv. Mater. *37*, 2414889. https://doi.org/10.1002/adma.202414889.

79. Wang, B., Cai, H., and Shen, S. (2019). Single metal atom photocatalysis. Small Methods *3*, 1800447. https://doi.org/10.1002/smtd.201800447.

80. Waele, V.D., Poizat, O., Fagnoni, M., Bagno, A., and Ravelli, D. (2016). Unraveling the key features of the reactive state of decatungstate anion in hydrogen atom transfer (HAT) photocatalysis. ACS Catal. *6*, 7174–7182. https://doi.org/10.1021/acscatal.6b01984.

81. Didarataee, S., Suprun, A., Joshi, N., and Scaiano, J.C. (2024). NIR phosphorescence from decatungstate anions allows the conclusive characterization of its elusive excited triplet behaviour and kinetics. Chem. Commun. *60*, 1896–1899. https://doi.org/10.1039/D3CC06282A.

82. Texier, I., Delouis, J.-F., Delaire, J.A., Giannotti, C., Plaza, P., and Martin, M.M. (1999). Dynamics of the first excited state of the decatungstate anion studied by subpicosecond laser spectroscopy. Chem. Phys. Lett. *311*, 139–145. https://doi.org/10.1016/S0009-2614(99)00803-9.